



## Core Scale Modelling of CO<sub>2</sub> Flowing: Identifying Key Parameters and Experiment Fitting

Jin Ma, Désirée Petrilli, Jean-Charles Manceau, Ruina Xu, Pascal Audigane,  
Luo Shu, Peixue Jiang, Yves Michel Le-Nindre

### ► To cite this version:

Jin Ma, Désirée Petrilli, Jean-Charles Manceau, Ruina Xu, Pascal Audigane, et al.. Core Scale Modelling of CO<sub>2</sub> Flowing: Identifying Key Parameters and Experiment Fitting. Energy Procedia, 2013, 37, pp.5464-5472. 10.1016/j.egypro.2013.06.466 . hal-03653136

**HAL Id: hal-03653136**

**<https://brgm.hal.science/hal-03653136>**

Submitted on 27 Apr 2022

**HAL** is a multi-disciplinary open access archive for the deposit and dissemination of scientific research documents, whether they are published or not. The documents may come from teaching and research institutions in France or abroad, or from public or private research centers.

L'archive ouverte pluridisciplinaire **HAL**, est destinée au dépôt et à la diffusion de documents scientifiques de niveau recherche, publiés ou non, émanant des établissements d'enseignement et de recherche français ou étrangers, des laboratoires publics ou privés.

GHGT-11

## Core scale modelling of CO<sub>2</sub> flowing: identifying key parameters and experiment fitting

Jin Ma<sup>a,b</sup>, Désirée Petrilli<sup>a,b</sup>, Jean-Charles Manceau<sup>a</sup>, Ruina Xu<sup>b</sup>, Pascal Audigane<sup>a</sup>, Luo Shu<sup>b</sup>, Peixue Jiang<sup>b</sup>, Yves Michel Le-Nindre<sup>a</sup>

<sup>a</sup>BRGM, Water Division, 3, av. Claude Guillemin BP 36009, 45 060 Orléans Cedex 2, France

<sup>b</sup>Department of Thermal Engineering, Tsinghua University, Beijing 100084, China

### Abstract

In this study, we propose to evaluate CO<sub>2</sub>-brine characteristics using core flooding experiment results with magnetic resonance (MR) imaging and a 1D numerical modelling approach along with a perspective on the role of CO<sub>2</sub>-brine characteristics on storage efficiency at the reservoir scale. MRI can be used to understand the pore structure and the flow characteristic of the drainage process more directly. The relative permeability curve which is the key parameter to field scale simulation can be obtained by the experiments. 1D numerical modelling is conducted to understand the results observed experimentally and the associated processes by using the parameters measured during the experiments. The modelling can explain the observed differences with the experiment through a sensitivity analysis and propose several set of parameters allowing a good match between experiments and models (history matching). It is shown that the combination method between the experiments and the modelling is a suitable method to understand the mechanism of CO<sub>2</sub> geological storage. Moreover, the experiments can provide the validation to the modelling which is the important tool to predict the CO<sub>2</sub> migration underground.

© 2013 The Authors. Published by Elsevier Ltd.  
Selection and/or peer-review under responsibility of GHGT

Keywords: Experimental multiphase flow, Magnetic Resonance (MR) imaging, Multiphase flow modelling, capillary and relative permeability laws

### 1. Introduction

To evaluate the storage efficiency of a geological formation a detailed characterization of the intrinsic properties of the rock like permeability and porosity is required. In addition, the characteristics of the gas and liquid phase flow properties like relative permeability and capillary pressure remain crucial. Technologies to measure such properties have been largely developed in the oil and gas industry with laboratory experiments. The laboratory experiments consists in co-injecting CO<sub>2</sub> and brine at different ratio into a rock core previously collected from exploration wells on the field until the pressure and flow rate at the outlet stabilize. When combined with computed tomography (CT) scanner or magnetic

\* Corresponding author. Tel.: +xxx ; fax: +xx .

E-mail address:

resonance (MR) imaging techniques these systems have the added capacity of measuring and visualizing the fluid saturation and porosity at the sub-core scale. Numerical modelling of such experiment allows for an extrapolation of the CO<sub>2</sub> flow and injectivity at the field scale. Regarding CO<sub>2</sub> geological storage few applications can be found in the scientific literature <sup>[1]</sup>. Evaluating in three dimensions (3D) the heterogeneous CO<sub>2</sub>-brine characteristics of a porous core during flooding experiments remains a high challenging objective with a substantial cost. In this study, we propose to evaluate CO<sub>2</sub>-brine characteristics using core flooding experiment results with MR and a 1D numerical modelling approach along with a perspective on the role of CO<sub>2</sub>-brine characteristics on storage efficiency at the reservoir scale. Our aims are (i) to understand the results observed experimentally and the associated processes by using the parameters measured during the experiments (ii) to explain the observed differences through a sensitivity analysis and (iii) to propose several set of parameters allowing a good match between experiments and models (history matching). We based our approach on a laboratory experiment conducted on Berea sandstone samples and using the multiphase flow code TOUGH2 developed by the Lawrence Berkeley National Laboratory in California, USA <sup>[2]</sup>. The 1D approach offers a very fast and easy way for evaluating influences of flow properties on CO<sub>2</sub> mobility and also for conducting sensitivity analysis. On the other hand, it requires a careful analysis of the results to not bias interpretation because of the geometrical simplification and we will also assess the limitations of such approach on several aspects. The first section will describe the experimental set up and results. The second section will describe the 1D model approach. End capillary effect, hysteresis and strategy for optimizing the matching on experimental data will be described and discuss.

## 2. Experimental Approach

### 2.1. Experimental System

The experimental facility setup for the investigation of two-phase core flooding experiments is presented in Fig. 1. The core-holder with core sample is placed horizontally inside a mini magnetic resonance (MR) device. Two pumps were used to inject CO<sub>2</sub> and pure water with a set flow rate. The two fluids were at the same pressure and temperature and mixed before reaching the inlet of the test section and flooding through the core sample. Fluorocarbon oil was injected into the interlayer of core-holder to build up a confining pressure which can prevent the mixed fluid flow through the gap between the core sample and core-holder. The confining pressure should be 1.5-2 MPa higher than the system pressure.

Pressure transducers allow for the measurement of the pressure at the inlet and the outlet and also to measure the pressure drop (difference between the inlet and outlet). The temperature of the system was monitored with platinum resistors. Water flow meter provides the inlet water flow rate while a scale is used to measure the outlet water flow rate. The gas flow meter serves to measure the outlet CO<sub>2</sub> flow rate after the separator. The water saturation was imaged by MR technique as explained in the next sections. The experiment was performed as a steady-state process. The two-phase fluids are assumed immiscible and incompressible. The basic theory is 1D-Darcy interstitial flow theory. The experiment was performed with constant total volume flow rate. The two fluids were injected into the test section at a particular ratio.

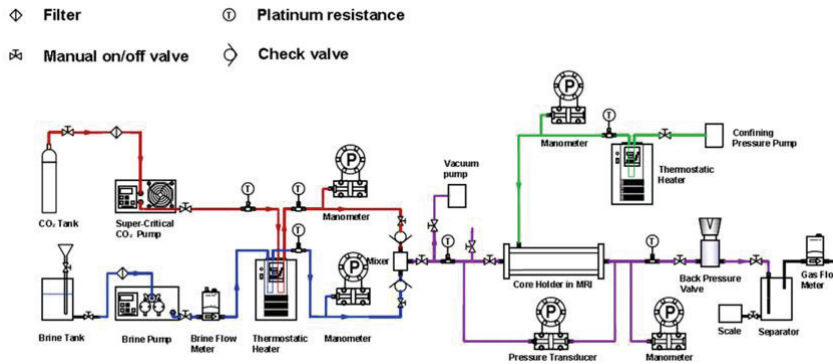


Fig. 1 Schematic of the experimental system for two-phase core flooding experiments

## 2.2. Experimental results

### 2.2.1. MR Measurements

The water content is measured by MR and weight measurement. MR can measure the water content directly keeping the core in the apparatus. The MR technique estimates the porosity at 22.02% with 0.08% as the relative error, while the scale method gives a porosity value of 21.53% with 2.58% as the relative error. Previous measurements using mercury intrusion technique estimated a porosity value of the core sample at 22.1% in good agreements with our measurements.

Effective porosity is calculated by using the relaxation time curve deduced from MR measurement. In order to understand MR contrast, it is important to have some understanding of the time constants involved in relaxation processes that establish equilibrium following radio frequent (RF) excitation.  $T_2$ -weighted imaging relies upon local de-phasing of spins following the application of the transverse energy pulse; the transverse relaxation time is termed "Time 2" or  $T_2$ , typically < 100 ms for tissue. Application of such method in geological applications [3] allows for characterizing the size of the pores in which water saturation is measured. The bigger  $T_2$  is, the bigger the pore is. The distribution and fraction of different pore sizes can be measured using the  $T_2$  curve. The  $T_2$  curve can be divided into three different parts: the clay bound water (irreducible water), the capillary irreducible water and the movable water. The capillary irreducible water and the movable water are considered as representative of the effective porosity. Fig. 2a is the  $T_2$  curve calculated from the experiment. The black curve is for water saturated state, and the red curve is for the core holder only. The effective porosity 20.14%, which means 91.48% of the pores can be considered as 'effective pores', while the movable water porosity is 19.81%.

### 2.2.2. Relative permeability and water saturation

The experiment was performed at 298K and 10MPa, while an imbibition process after drainage in the same conditions. The volumetric flow ratio of  $\text{CO}_2:\text{H}_2\text{O}$  varied as 49:1, 19:1, 3:1, 1:1, 1:3, 1:19, keeping the total flow rate constant as 2 ml/min. Fig. 3 is the relative permeability versus water saturation curve. The blue spots are the water relative permeability from the experiment which increases with the water saturation. The red spots are the  $\text{CO}_2$  relative permeability from the experiment which decreases instead. At the beginning of imbibition, for the ratio of  $\text{CO}_2:\text{H}_2\text{O}=49:1$ , the two-phase flow was not easy to get stable. It is because when the water fraction is extremely low, the component of the fluid is not constant due to the dissolution and diffusion.

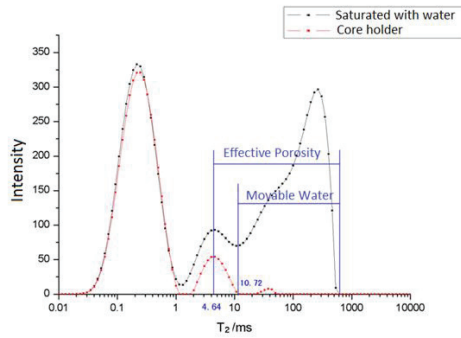


Fig. 2  $T_2$  curve schematic of effective porosity and movable water state of the core sample used in the experiment

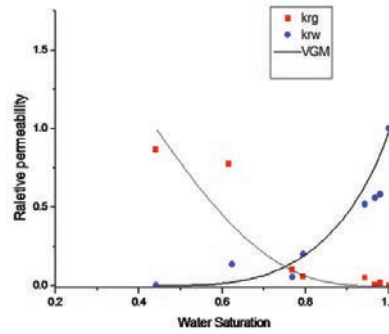


Fig. 3 Relative permeability variation with water saturation

The irreducible water after drainage from the experiment is 44.1%, and the residual gas saturation is about 4%. The residual gas saturation turns out relatively low, because pure water is used in the experiment and residual  $\text{CO}_2$  dissolves into pure water constantly.

The Van Genuchten-Mualem model (Mualem, 1976 ; van Genuchten, 1980) is used to fit the experimental result, which is as follow:

$$K_{rl} = \sqrt{S^*} \{1 - [1 - (S^*)^{1/m}]^m\}^2, \quad K_{rg} = (1 - \hat{S})^2 (1 - \hat{S}^2)$$

$$\text{where } S^* = \frac{(S_l - S_{lr})}{(1 - S_{lr})}, \quad \hat{S} = \frac{(S_l - S_{lr})}{(1 - S_{lr} - S_{gr})}.$$

$S_l$  is the water saturation,  $S_{lr}$  is the irreducible water saturation and  $S_{gr}$  is the residual gas saturation. According to the experimental results, the exponent  $m$  is 0.66. The fitting result is shown as the black line in Fig. 3.

### 3. Numerical simulation of the displacement of $\text{CO}_2$ injection into the water saturated rock

For the numerical modelling, we used the multiphase fluid flow transport code TOUGH2<sup>[2]</sup> including the EOS module ECO2N. The aim of this study is to understand the results observed experimentally and the associated processes. The parameters measured during the experiments are used for the numerical simulations (called “base case” in the following) and we observe how close simulations and experimentations results are using additional alternative cases as described below.

#### 3.1. Physical model, and base case presentations

Considering the small size of the core and the absence of information regarding the heterogeneity of the core and of the transversal variability of the parameters measured, we decided to use a simple 1D mesh using the core dimensions. The length of the saturated rock along the flow direction is 50 mm and was divided into 20 slices (cells). The sectional area is 24mm×24mm. We design a base case which strictly follows the results given by the experiments. The permeability was measured by the core supplier (650 mD; a little different from the value we measured – 512mD). The porosity was also given by the supplier and confirmed experimentally at 0.22. The van Genuchten relative permeability laws parameters for  $\text{CO}_2$  flooding were estimated according to the experiment at  $m=0.66$  and  $S_{gr}=0.44$ . The residual gas saturation  $S_{gr}$ , is set to 0.0001 during the drainage phase and to 5% (measured at 0.04) for the imbibition stage.

No experimental data were available for capillary pressure. We used data from Krevor et al. [4], who performed mercury injection capillary pressure and obtained parameters for Brooks and Corey capillary pressure model. Adapted to van Genuchten model, as  $P_{cap} = -P_o((S^*)^{1/m} - 1)^{1-m}$ , we obtained the following parameters:  $m=0.425$ ,  $S_{lr}=0.11$  and  $P_o=2000\text{Pa}$ . No difference between the two stages (hysteresis phenomenon) was taken into account for capillary pressure in a first approach. Constant thermo-physical properties at 298 K were assumed for  $\text{CO}_2$  and water. The boundary conditions were fixed with respect to the experiment: a constant injection rate (100%  $\text{CO}_2$  or  $\text{CO}_2$ -brine mixing) was applied at the inlet of the core (2 ml/min) and a constant pressure was set at the outlet (10 MPa). For initial condition, the rock sample was at 10 MPa and 25°C and 100% saturated by water. Then the irreducible water saturation was obtained after drainage. For the imbibition process, various water and  $\text{CO}_2$  injection ratios were simulated one by one, with water fraction increasing.

### 3.2. Results of base case

#### 3.2.1. Pressure difference

The pressure differences between the core inlet and outlet are displayed against gas saturation in figure 4. The black line represents the simulation result and the red spots represent the experimental result. We observe these two results can agree with each other quite well. It is due to the relative permeability curve which we used in the simulation can describe the experiment properly. The numerical results given by TOUGH2 simulation can complete the discrete experimental results. Fig.4 shows the maximum pressure difference occurs around the water saturation is 0.85-0.9. Actually, if we modify the relative permeability curve in the simulation, the pressure difference curve showed in Fig. 4 will be changed.

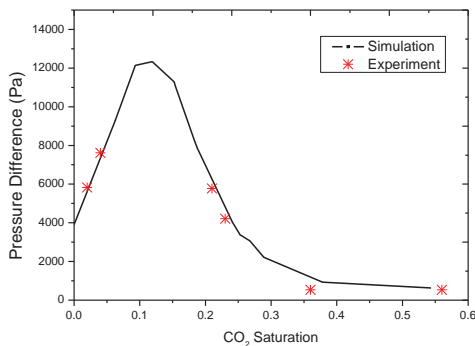


Fig 4. Pressure difference varies with water saturation

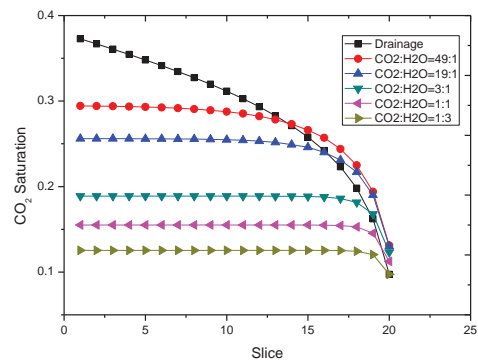


Fig 5. Gas saturation profiles along the core after steady state for the drainage and imbibition stages

#### 3.2.2. $\text{CO}_2$ saturation and distribution

Figure 5 depicts the gas saturation profiles along the core after steady state during the drainage and imbibition stages (for different gas to liquid ratios). For the drainage process, even after a long simulation time, no drying out is observed. This can be explained by figure 6. The constant pressure at the core outlet being is applied with an infinite volume of water at the last slice of the model, the water flow is unlimited and we obtain a real steady state. In reality, water flow is limited and sooner or later a drying out should be observed. The capillary effects makes the gas pressure gradient positive while the liquid pressure gradient negative, which leads to a water flow opposite to the gas flow.

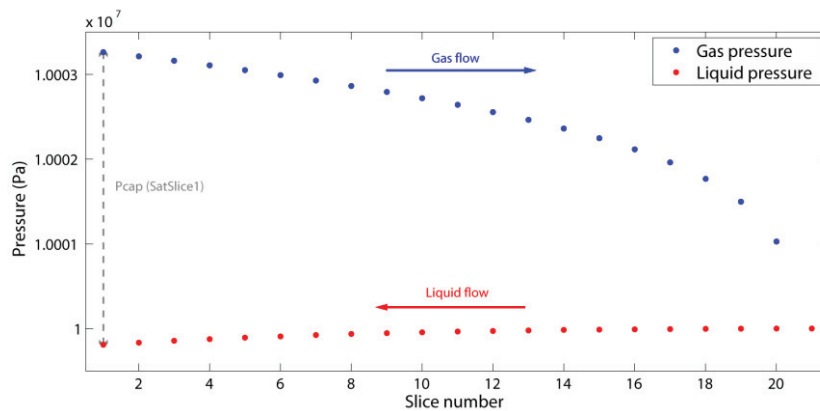


Fig 6. Gas and liquid pressure along the core during drainage at steady state: explanation of the counter-flow

During the imbibition process showed in Fig. 5, for each gas to liquid ratios, a saturation plateau on the main part of the core. The numerical side effects are also obtained during imbibition and explain the gas saturation drop at the end of the profile. This allows an estimation of the side effects significance: they have a relatively large impact when a majority of gas is injected but a lower one when mainly water is injected.

### 3.3. Sensitivity analysis

The base case simulations show some discrepancies between the experiment and the numerical model. Given the uncertainties for a high number of input parameters in the model, we perform a sensitivity analysis on key-parameters in order to evaluate the consequences of these uncertainties. The choice of the key-parameters has been based on the observations mentioned in the previous section. We then decided to change the capillary pressure curve ( $P_0$  in van Genuchten capillary pressure law) and the relative permeability curve, and then analyse the sensitivity.

#### 3.3.1. Capillary pressure curve

The values considered in the base case were adapted from Krevor et al. (2012). However, capillary pressure parameters are unknown in our experiment. In a similar work on Berea sandstone, Shi et al. (2011) proposed to use van Genuchten capillary pressure law parameters obtained for water/air system for the brine/ $\text{CO}_2$  system and used the following parameters:  $m=0.425$ ,  $S_{lr}=0.09$  and  $P_0=20000\text{Pa}$ . to check the effects of the capillary pressure variation on the modeling, other  $P_0$  were selected:  $P_0=200\text{ Pa}$  and  $P_0=20000\text{ Pa}$ . The capillary pressure curves from literature and used in this study are depicted in Fig. 7a. Fig. 7b shows the pore size distribution of the core sample of our study and the one from Shi's study. We observe the peak (or average) of the pore diameter from our sample is bigger than Shi's. A smaller pore size leading to a higher capillary strength (Seol and Kneafsey, 2008), the capillary strength should be lower than the one considered by Shi et al. (2012).

The simulation results are showed in figure 8, in which a) is for the  $P_0=200\text{ Pa}$  case and b) is for the  $P_0=20000\text{ Pa}$  case. During the drainage stage, one can observe major changes due to  $P_0$  modifications. The profile is indeed highly different. The gas saturation is lower when the capillary effects are stronger and increases when  $P_0$  is lowered. For the case  $P_0=200\text{Pa}$ , we even observe a drying out for the two last time steps. This can also be explained by the backflow/non-backflow of water. When the capillary pressure decreases, the negative pressure difference for water will fade out. As the backflow disappeared, the dry-out zone occurs. During imbibition, when a significant fraction of water is injected, there is no major difference between the profiles except a higher influence of the capillary end effects.



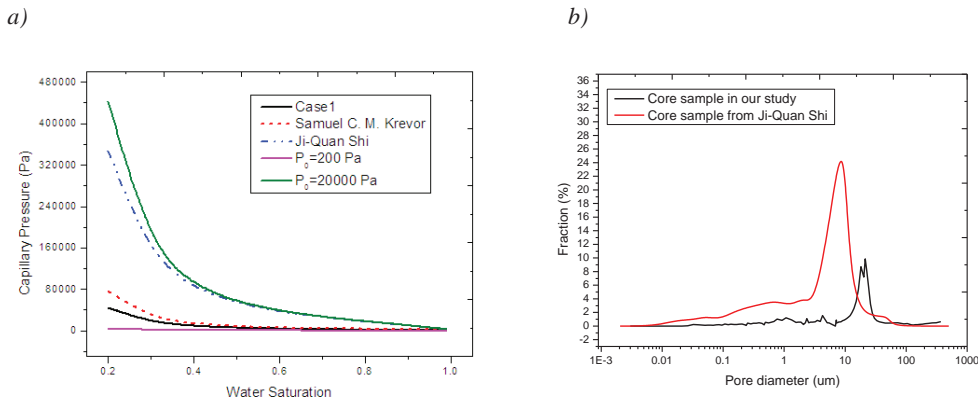


Fig 7. a) Capillary pressure curves with  $P_0=200$  Pa and  $P_0=20000$  Pa, compared with the base case, b) Comparison of pore size distribution of the core sample in our study and the literature

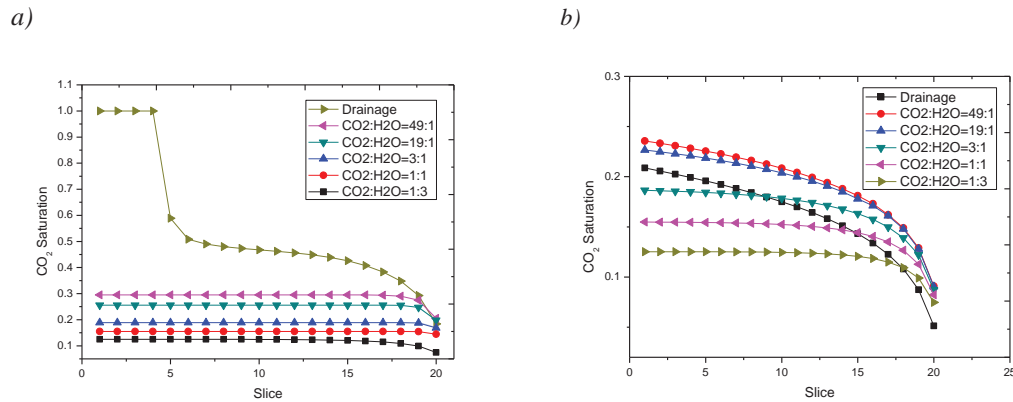


Fig 8. a) Gas saturation profiles along the core with  $P_0=200$  Pa, b) Gas saturation profiles along the core with  $P_0=20000$  Pa

### 3.3.2. Relative permeability curve

The relative permeability curve is significant for simulation of two phase flow. In this study, we changed irreducible water saturation ( $S_{lr}$ ) and residual gas saturation ( $S_{gr}$ ) separately. Figure 9 shows the modified curve for  $S_{lr}=0.15$  and  $S_{gr}=0.15$ , compared with the original curve we obtained from the experiment and used in the base case (Case 1).

The simulation results are shown in figure 10, in which a) is for the  $S_{lr}=0.15$  case and b) is for the  $S_{gr}=0.15$  case. We can observe that decreasing the irreducible water saturation leads to an increase in the average saturation in the core both in drainage and in imbibition.

For the residual gas, we recall that non-zero residual gas saturation was considered for imbibition. This value represents the gas quantity residually trapped due to capillary forces. When we decreased the  $S_{gr}$ , we find it will be more difficult to change the gas saturation by varying the injection ratio. On the other hand, since we used two different imbibition curves, there is a significant change between the gas saturation curve of the drainage state and the injection ratio of  $\text{CO}_2\text{-H}_2\text{O} = 49:1$  state.



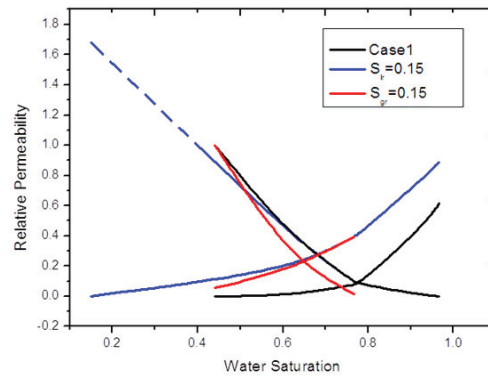


Fig 9. Relative permeability curves with  $S_{lr}=0.15$  and  $S_{gr}=0.15$ , compared with the base case

a)

b)

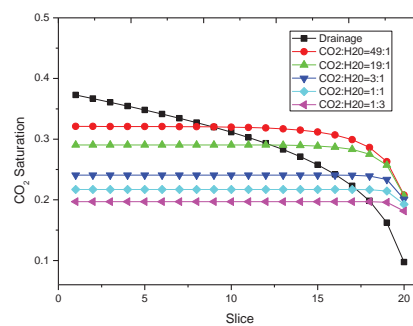
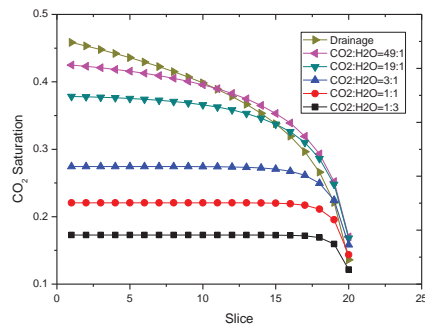


Fig 10. a) Gas saturation profiles along the core with  $S_{lr}=0.15$ , b) Gas saturation profiles along the core with  $S_{gr}=0.15$  Pa

#### 4. Conclusion

In this study, we propose to evaluate  $\text{CO}_2$ -brine characteristics using core flooding experiment results with MR imaging and a 1D numerical modelling approach along with a perspective on the role of  $\text{CO}_2$ -brine characteristics on storage efficiency at the reservoir scale. MR imaging can be used to understand the pore structure and the flow characteristic of the drainage process more directly. The relative permeability curve which is the key import parameter to field scale simulation can be obtained by the experiments. A simple 1D numerical modelling approach is proposed to understand better experimental results and associated processes with regards to the parameters measured during the experiments. Through the sensitivity analysis, we propose several set of parameters allowing a good match between experiments and models (history matching). It is shown that the combination of experimental and modelling approach allows for a better understanding of the mechanisms which controls multiphase flow processes during  $\text{CO}_2$  geological storage.

#### Acknowledgements

This project was supported by the National Natural Science Foundation of China (Grant No. 50906043), Major Project of Beijing Natural Science Foundation (No. 3110001) and the Tsinghua University Initiative Scientific Research Program. This research was also supported/sponsored by the framework of the CEFCEET (Centre Franco-Chinois de l'Environnement et de l'Energie de Tsinghua)

which constitutes a real networking cooperation for education and research exchanges between France and China based on an initiative of the French Ministère de l'Éducation Nationale..

## References

- [1] Müller N. Supercritical CO<sub>2</sub>-Brine Relative Permeability Experiments in Reservoir Rocks—Literature Review and Recommendations. *Transp Porous Med* 2011; 87:367–383.
- [2] Pruess, K., Oldenburg, C.M., Moridis, G.: TOUGH2 User's Guide, Version 2.0. Report LBNL-43134. Lawrence Berkeley National Laboratory, Berkeley, CA, USA (1999).
- [3] Gingras M.K., MacMillan, B., Balcom, B.J. Saunders, T., Pemberton, S.G., Using Magnetic Resonance Imaging and Petrographic Techniques to Understand the Textural Attributes and Porosity Distribution in Macaronichnus-Burrowed Sandstone *Journal of Sedimentary Research*, vol. 72, no. 4, pp. 552-558, 2002.
- [4] Krevor, S.C.M., Pini, R., Zuo, L., Benson S.M.: Relative permeability and trapping of CO<sub>2</sub> and water in sandstone rocks at reservoir conditions. *Water Resources Research* 48, W02532 (2012) doi:10.1029/2011WR010859, (2012).
- [5] Kopp A, Class H, Helmig R. Investigations on CO<sub>2</sub> storage capacity in saline aquifers Part 1. Dimensional analysis of flow processes and reservoir characteristics. *Int J GreenH Gas Con* 2009; 3:263 – 276.
- [6] Shi JQ, Xue, Z, Durucan, S, Supercritical CO<sub>2</sub> core flooding and imbibition in Tako sandstone—Influence of sub-core scale heterogeneity. *Int J GreenH Gas Con* 2011; 5:75-87.
- [7] Pini, R., Krevor, S., Benson, S., Capillary pressure and heterogeneity for the CO<sub>2</sub>/water system in sandstone rocks at reservoir conditions, *Advances in Water Resources*, 38, 48-59, (2012).
- [8] Lenhard, R.J., Parker, J.C.: A model for hysteretic constitutive relations governing multiphase flow – 2. Permeability-saturation relations. *Water Resour. Res.* 23(12), 2197-2205 (1987)